



Alkali-Activated Binders From Waste Incinerator Bottom Ashes and Metakaolin Reinforced by Recycled Carbon Fiber Composites

Stefania Manzi^{1*}, Isabella Lancellotti², Giulia Masi¹ and Andrea Saccani¹

¹Department of Civil, Chemical, Environmental and Materials Engineering, University of Bologna, Bologna, Italy, ²Department of Engineering "Enzo Ferrari", University of Modena and Reggio Emilia, Modena, Italy

OPEN ACCESS

Edited by:

Patricia Krawczak,
IMT Lille Douai, France

Reviewed by:

Nassim Sebaibi,
École Supérieure d'Ingénieurs des
Travaux de la Construction, France
Girts Bumanis,
Riga Technical University, Latvia

*Correspondence:

Stefania Manzi
stefania.manzi4@unibo.it

Specialty section:

This article was submitted to
Structural Materials,
a section of the journal
Frontiers in Materials

Received: 15 July 2020

Accepted: 06 October 2020

Published: 12 November 2020

Citation:

Manzi S, Lancellotti I, Masi G and
Saccani A (2020) Alkali-Activated
Binders From Waste Incinerator
Bottom Ashes and Metakaolin
Reinforced by Recycled Carbon
Fiber Composites.
Front. Mater. 7:583400.
doi: 10.3389/fmats.2020.583400

In view of creating low-impact materials for the building industry, the fostering of alkali-activated binder gains high importance. Metakaolin can successfully be activated with alkalis at room temperature, but the contemporary use of wastes to create mixed binders can further increase the environmental benefits. Bottom ashes obtained from the incineration of municipal solid wastes have been tentatively mixed in different amounts to develop matrix with acceptable mechanical properties, which still can be cured at room temperature. Moreover, scraps obtained from the production of epoxy/carbon fiber composites are employed as a reinforcing phase. No chemical or physical treatments have been used to modify the epoxy/carbon fiber wastes, apart from size reduction, thus minimizing the overall economic and energy impact of the process. The workability, physical and mechanical properties, microstructure, and porosity of the obtained materials are investigated. Up to a 50 weight percent of bottom ashes from municipal solid waste incineration can be mixed with metakaolin. Fibers still embedded in the epoxy matrix disclose a fair interaction with the matrix, thus managing to increase flexural strength, toughness, and dimensional stability without decreasing the compressive strength.

Keywords: building materials, carbon fibers composites wastes, bottom ashes, recycling, alkali-activated materials

INTRODUCTION

Municipal waste incineration can be used as a waste handling solution. This process can recover energy, exploiting the heat of combustion of the organic fraction of the waste and allows the overall reduction of the volume of wastes, consequently decreasing landfilling depletion. As a drawback, the process itself generates solid wastes, defined as fly ash and bottom ash. Bottom ashes from municipal solid waste incineration have some remarkable characteristics. They contain negligible amounts of toxic elements, have high amorphous fraction, and are largely composed of silica and aluminium oxides. These characteristics have already attracted interest for their use in producing new glass compositions (Saccani et al., 2001) or building materials, especially their pozzolanic activity in traditional Portland cement composites (Saccani et al., 2005; Li et al., 2012; Kuo et al., 2013; Tang et al., 2016; Chen and Yang, 2017; Chen et al., 2019). In recent years, a new class of binders has been investigated, characterized by a lower carbon dioxide footprint than Portland cement, that is, alkali-activated materials (De Vargas et al., 2011; Sun and Vollpracht, 2019). There are a set of inorganic

phases showing amorphous or semicrystalline structure formed by a three-dimensional network of AlO_4 and SiO_4 tetrahedra. They are obtained from a chemical reaction between a binding component (the source of aluminosilicates) and an alkaline activator, usually a blend of caustic alkalis or alkaline salts. For their synthesis, raw materials such as metakaolin, calcined clays, or industrial wastes, such as fly ash or slags, have been used (Boca Santa et al., 2016; Borges et al., 2016; Logesh Kumar and Revathi, 2016; Boca Santa et al., 2017; Bai et al., 2019). Bottom ashes from municipal solid waste incineration can also have an application in these materials because they can be alkali activated when mixed with metakaolin (Lancellotti et al., 2013; Lancellotti et al., 2014; Lancellotti et al., 2015; Silva et al., 2017; Wongsu et al., 2017; Huang et al., 2018). They cannot be used alone as precursor because the amount of Al_2O_3 is too low and the higher amount of calcium can change the chemistry of the polymerized network that is formed from alkali activation with the creation of C-A-S-H gels (Borges et al., 2016; Zhu et al., 2018). The alkali activation of this class of materials can take place at different temperatures (Rovnanik, 2010). The most interesting results are obtained from the activation at room temperature (Aredes et al., 2015). Other wastes can be activated only at high temperatures (Sha et al., 2020). It is thus important to verify the mechanical properties of the mixed binders when cured at room temperature.

However, the main problems concerning alkali-activated materials are their complete brittleness and their low dimensional stability. Both defects can be mitigated by modifying the composites through fibers addition, as reported in the literature (Uddin and Shaikh, 2013; Vilaplana et al., 2016; Al-Mashhadani et al., 2018; Bhutta et al., 2018; Luna-Galiano et al., 2018; Akono et al., 2019; Farooq et al., 2019). Waste carbon fibers (CF), embedded in a thermosetting polymer matrix, virtually have high mechanical properties. Either they can be derived from post-user dismissed items or they can be the pre-preg offcuts derived from the manufacturing process. Bare fibers can be recovered, eliminating the thermosetting matrix by means of high thermal treatments or selective chemical dissolution. Both the processes imply energy consumption and waste production. The direct use of scraps has been proposed in different matrixes, such as Portland cement, alkali-activated fly ashes, and pure metakaolin. Positive results have been obtained in terms of increased flexural strength and toughness, implying that the presence of a polymeric interphase (epoxy resin) between the fiber and the ceramic matrix still enables a positive interaction between fiber and matrix (Saccani et al., 2019). It seems thus interesting to evaluate the effect of CF/epoxy scraps also in the alkali-activated systems where metakaolin is partially substituted by bottom ashes from municipal solid waste incineration. The mix design has been investigated focusing on the workability of fresh mixtures, microstructure (i.e., fibers dispersion and porosity), flexural strength, and toughness. A room temperature curing has been studied, being the lowest energy-consuming treatment. In case these materials should prove to have acceptable mechanical properties, which is the main scope of the research, they could provide potentially high environmental benefit because they could enable the simultaneous recycling of

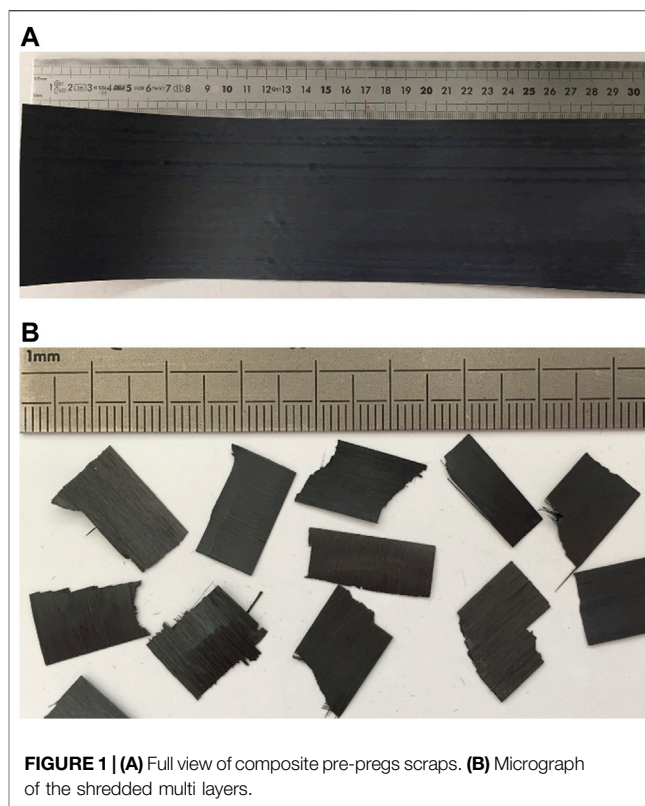


FIGURE 1 | (A) Full view of composite pre-pregs scraps. **(B)** Micrograph of the shredded multi layers.

TABLE 1 | Composition of the raw materials (wt%).

Material	SiO_2	Al_2O_3	Na_2O	K_2O	CaO	MgO	Fe_2O_3	TiO_2	MnO	LOI
Metakaolin	53.5	41.9	0.0	2.6	0.0	0.0	1.4	0.6	0.0	0.0
Bottom ash	49.5	9.4	5.7	1.4	17.5	2.9	4.9	0.9	0.2	4.9

different wastes, reducing the amount of metakaolin and virgin carbon fibers to be used. The first issue eliminates the thermal treatments of aluminosilicate precursor that are necessary, thus avoiding CO_2 emissions, and the second one would prevent scrap damping and avoid virgin fiber production. Indeed, the complete life cycle assessment of the derived material should be carried out, a process that is however beyond the aims of this study that merely faces the technical problems related to the material performance upon modification.

EXPERIMENTAL

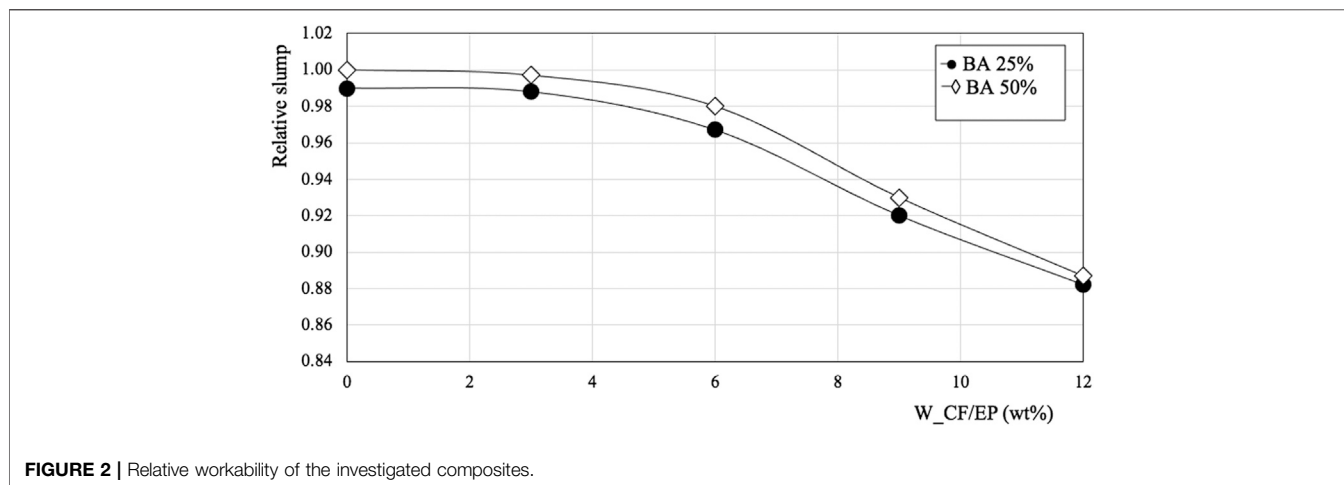
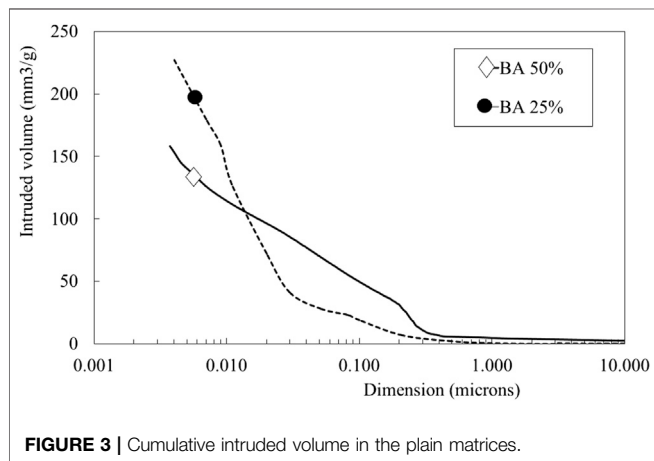
Composites Waste Scraps

Pre-preg offcuts derived from the production of CF/epoxy (hereafter defined as $W_{\text{CF/EP}}$) composites have been used. The as-received scraps had an almost rectangular shape with side dimension ranging from 10 to 40 cm (Figure 1A shows an example). They were made of multiple CF/epoxy impregnated layers with an average thickness ranging from 150 to 450 μm .

TABLE 2 | Formulation of composites.

Sample	Metakaolin (g)	BA (g)	NaOH 8M (ml)	Na ₂ SiO ₃ (ml)	W_CF/EP (g)	w/b ratio
BA25-W_CF/EP0	75	25	25	60	0	0.36
BA25-W_CF/EP3	75	25	25	60	3	0.36
BA25-W_CF/EP6	75	25	25	60	6	0.36
BA25-W_CF/EP9	75	25	25	60	9	0.36
BA25-W_CF/EP12	75	25	25	60	12	0.36
BA50-W_CF/EP0	50	50	16	40	0	0.28
BA50-W_CF/EP3	50	50	16	40	3	0.28
BA50-W_CF/EP6	50	50	16	40	6	0.28
BA50-W_CF/EP9	50	50	16	40	9	0.28
BA50-W_CF/EP12	50	50	16	40	12	0.28

BA, bottom ash; CF, waste carbon fibers; W_CF/EP, pre-preg offcuts derived from the production of CF/epoxy; w/b ratio: water/binder ratio.

**FIGURE 2** | Relative workability of the investigated composites.**FIGURE 3** | Cumulative intruded volume in the plain matrices.

The original multiple layer sheets were treated for 1 h at 130°C to complete the cross-linking reactions and then cut to obtain fibers bundles with the length of 13 ± 2 mm and lateral size ranging from 5 to 10 mm (**Figure 1B**). The amount of resin that surrounds the carbon fibers was evaluated by weight loss through the use of a TGA instrument (Thermogravimetric Analysis, Q50 Model TA Instruments) and was estimated as a 30 ± 8 wt%.

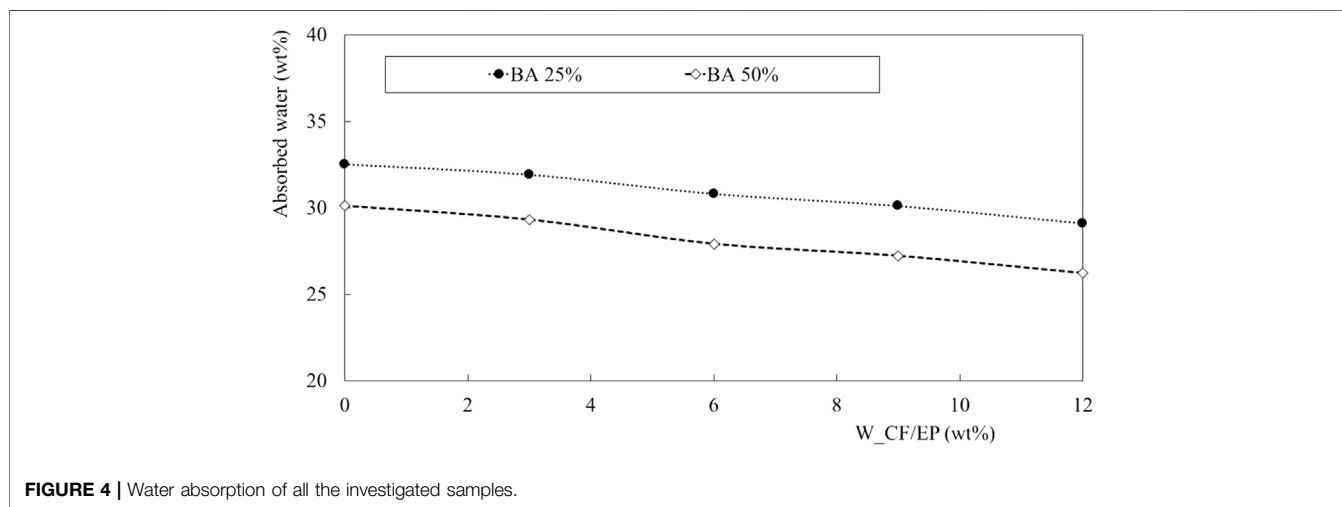
Binders

Metakaolin with a dimension lower than 75 μm was used as binder. Bottom ashes from municipal waste incineration, hereafter simply defined as BA, once collected by the company managing the disposal of ashes from different incinerator plants are submitted to beneficiation. The process involves ageing, grinding, and Fe and Al separation by means of magnetic and eddy current systems. After these treatments, BA are no more classified as waste according to the European Waste Code, but as secondary raw materials (end of waste). Final product was ball-milled and sieved through a 100 μm sieve to favor their homogeneous mixing with metakaolin and subsequent reactions. In details, metakaolin powders show the following parameters: $D_{10} = 1.40$, $D_{50} = 11.08$, and $D_{90} = 50.98$. For BA the values are as follows: $D_{10} = 1.81$, $D_{50} = 21.53$, and $D_{90} = 61.71$. Data have been derived by laser particle sizer Fritsch, Analysette 22. **Table 1** reports the chemical composition of both metakaolin and BA as derived by X-ray fluorescence (Philips PW 2004). Other detected elements, such as sulphur, phosphor, and chlorine, are not reported. Loss on ignition was determined after a 2 h treatment at 1,100°C. X-ray analysis was performed in order to evaluate the amorphous or crystalline nature of BA and to identify the crystalline phases present. From the analysis (not reported for brevity sake), the typical amorphous/

TABLE 3 | Classification of porosity in the investigated samples according to IUPAC.

Designation	Porosity range (nm)	BA 25% (mm ³ Hg/g) (%)	BA 50% (mm ³ Hg/g) (%)
Micropores	<1.25	n.d.	n.d.
Mesopores	1.25–25	156.0 (68.4)	67.0 (42.4)
Macropores	25–5,000	71.9 (31.5)	88.0 (55.7)
Directly accessible large pores	5,000–50,000	0.1 (0.0)	3.0 (1.9)
Total porosity	—	228.0 (100)	158.0 (100)

Pore size classification (percentage of porosity over the total specific volume of Hg is reported in brackets).



crystalline nature of the material is determined. Among the crystalline fraction, the main detected phase is α -quartz (α -SiO₂, JCPDF file 33-1161) followed by calcite (CaCO₃ JCPDF file 5-586), and aluminosilicates as albite (NaAlSi₃O₈ JCPDF file 10-393) and ghlenite (Ca₂Al(Al,Si)O₇ JCPDF file 35-755), thus reflecting the chemical analysis of a typical ash rich in calcium and sodium.

Activators

Sodium hydroxide reagent grade and sodium silicate solution, a viscous liquid produced for the cement industry with a water content of 57 wt% and a SiO₂/Na₂O ratio of 3, were used as alkaline activators.

Mixing Procedures and Compositions

Sodium hydroxide 8M solution and sodium silicate have been first mixed according to the quantities determined in previous experiments (Lancellotti et al., 2013; Lancellotti et al., 2014). The quantities added aimed primarily to obtain equal workability. Moreover, due to the higher content of Na in BA, less amount of sodium hydroxide and silicate are added. On account of the higher ratio of SiO₂/Al₂O₃ in BA, less silicate is added (Table 1). Afterward, metakaolin mixed with the different quantity of BA (25 or 50 wt%) was added. The workability was determined through the minislump test proposed by EN-ETC. No additional water has been added to the fiber-modified materials and consequently workability decreased as the amount of W_{CF/EP} increased. However, up

to the highest investigated quantity, it was still possible to effectively fill the moulds without creating macro-voids. W_{CF/EP} amounts were 3, 6, 9, and 12 wt% on the powders. Table 2 reports the mix design of the investigated materials. The dimension of the prepared samples during casting procedures was different on the basis of further characterizations. Prisms of 100 mm × 20 mm × 20 mm size were cast (nine for each composite composition) and cured for 28 days at 25 ± 1°C and 98 ± 1% relative humidity. Prisms of 250 mm × 25 mm × 25 mm were used to investigate the free-drying shrinkage vs time when samples were cured at 25°C and 35 ± 5% relative humidity.

Tests and Procedures

Water Absorption and Porosity

Water absorption has been evaluated according to the UNI 7699 Standard (UNI 7699, 2005) on three samples (100 mm × 20 mm × 20 mm) cured for 28 days. The cumulative open porosity and the size distribution of the porosities in samples without fibers (i.e., the plain matrixes formulated with 25 and 50 wt% of BA but without the fibers) have been evaluated by mercury intrusion porosimetry (MIP) equipped with a macropore unit (Thermo Scientific, Pascal 140 and 240). Measurements were conducted at 28 days of curing. MIP measurements performed on composite samples were not reliable or reproducible because of the small dimension of the tested specimens allowed and the unavoidable damage induced by specimen size reduction. Accordingly, they will not be reported.

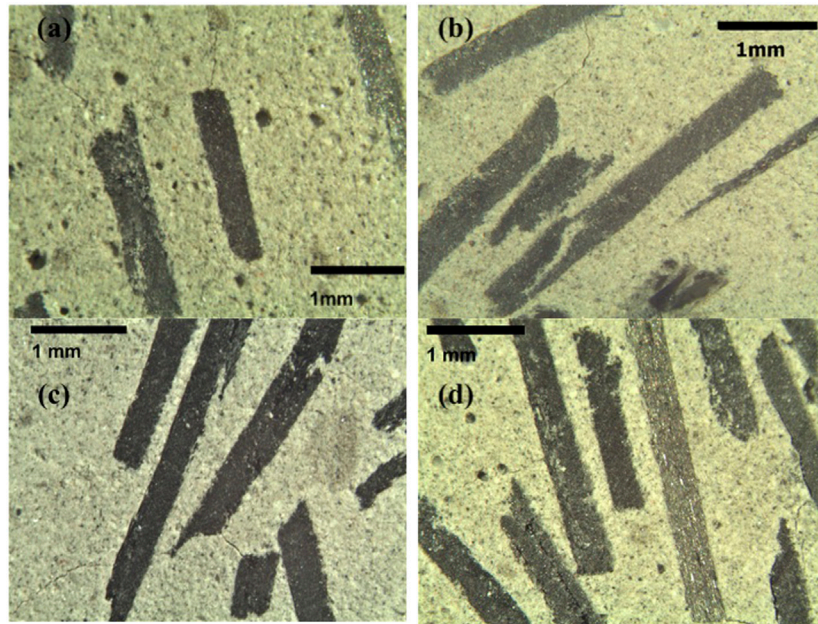


FIGURE 5 | Optical micrograph of BA25-W_CF/EP samples cross sections at 3 (A), 6 (B), 9 (C), and 12 (D) wt. amount of fibers at 20x.

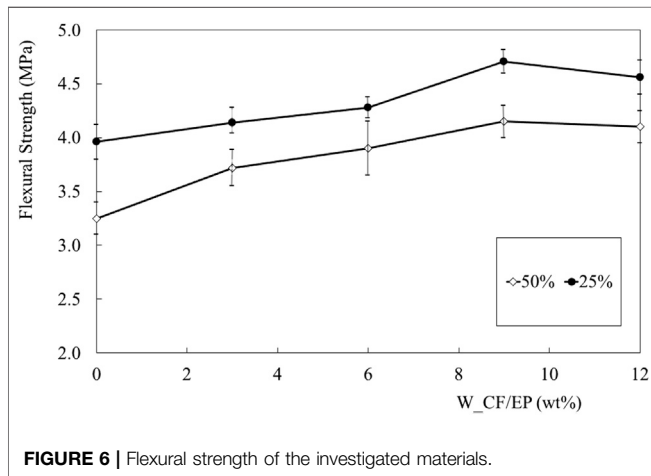


FIGURE 6 | Flexural strength of the investigated materials.

Mechanical Tests

Mechanical tests (three-point bending) were performed at room temperature with a relative humidity of $50 \pm 10\%$ by means of 100 kN Amsler Wolpert equipment, with a 5 mm/min displacement rate. Flexural strength values are reported as the average of six measurements. Compressive strength measurement was performed on both the prisms derived from the previous flexural test (12 measurements).

SEM Analysis

Morphological investigations were carried out on fractured surfaces of mortar samples sputtered by graphite by means of

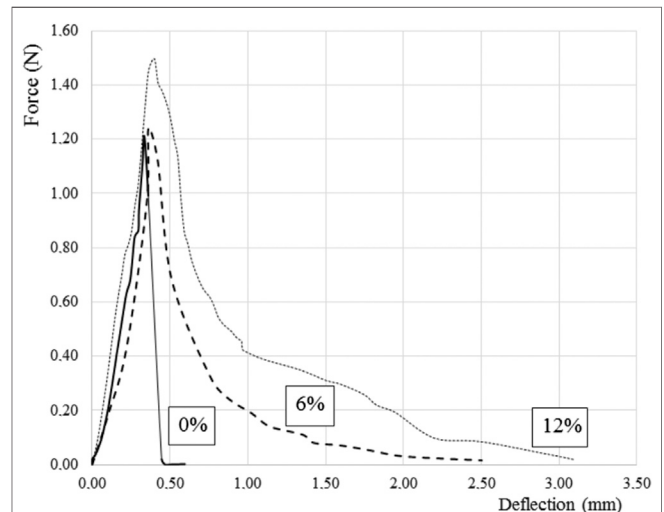


FIGURE 7 | Force vs deflection plot of specimens containing 50% of BA at different amounts of W_CF/EP.

electron scanning microscopy (ESEM, Quanta-200, FEI Co.), exploiting the signal collected by secondary electrons detectors. An accelerating voltage of 20 kV was applied.

Dimensional Stability

Dimensional stability has been evaluated according to the ASTM C1012/C1012M standards (ASTM C1012/C1012M, 2015) on three prismatic specimens of 250 mm × 25 mm × 25 mm cured at 25°C and $35 \pm 5\%$ relative humidity.

RESULTS

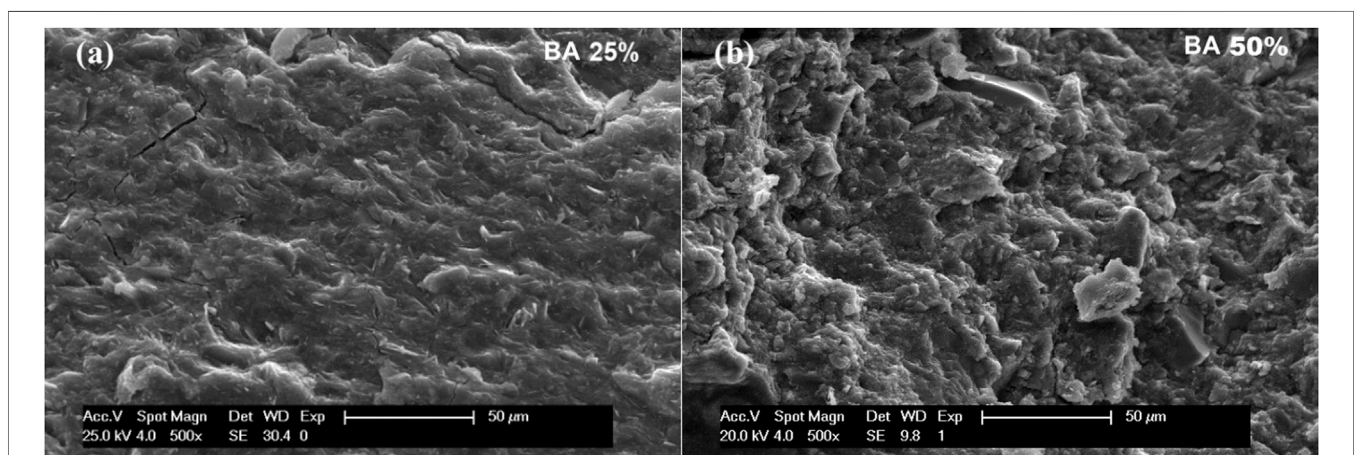
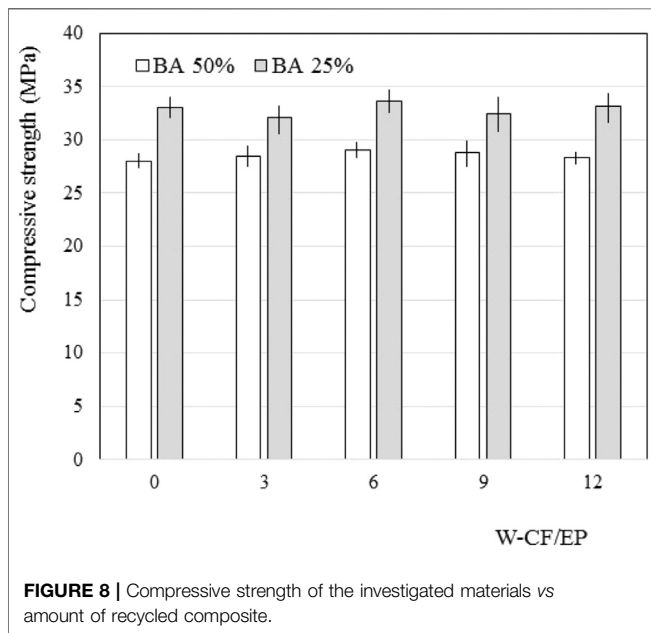
Figure 2 shows the relative workability of samples containing the different amounts of recycled composites, as well as the different amounts of BA. Standard deviations are not included for the sake of clearness because they almost coincide with the dimension of the symbols. While the effect of the different amounts of BA is negligible as desired, W_CF/EP addition progressively decreases this property. However, as underlined before, all mixtures could be easily cast without the formation of macrovoids. The decrease is partially related to the amount of water requested to wet the reinforcement surfaces. Although the composites scraps are no more flexible after the full-cross-

linking reaction, their small dimension prevents buckling phenomena.

Figure 3 shows the results of MIP analysis: the total intruded volume in the two different plain matrices is reported vs the pore dimension. The sample containing the lower amount of BA (25%) shows the highest overall porosity (228 mm³/g of intruded volume), with almost half of the pores having dimensions lower than 0.01 μm. BA 50% matrix shows a lower overall porosity (158 mm³/g of intruded volume), but the dimension of the pores is larger than that in the previous sample, mainly falling in the range from 0.4 to 0.01 μm. To get a detailed analysis of the results, **Table 3** reports the amount of pores divided in different ranges proposed by the IUPAC classification. The main differences are related to the mesopores and macropores that suggest similar observations as those previously proposed. In the BA 25% sample, no large pores (>5,000 nm) are detected, and the amount is quite limited in the BA 50% sample.

This can be explained by assuming that, in the applied curing conditions, the reactions involving the BA fraction are slower than those involving metakaolin, thus producing a lower amount of binding products or polymerized network only partially filling the larger voids, as found in other researches (Guo et al., 2017; Sha et al., 2020). Moreover, the presence of C-S-A-H product can change the porosity of the products. Consequently, although the w/b ratio in the BA 50% sample is lower, the capillary porosity is increased.

Figure 4 reports the water absorption of all the samples after 28 days of curing. The higher amount of BA slightly decreases the amount of absorbed water. Moreover, as the amount of recycled composite increases, values tend to decrease slightly at both the BA amounts. The percentage of absorbed water is usually linked to the overall volume of open porosity in the material. This result is also in accordance with the previous observation on the absence of large voids caused by the workability reduction. Moreover, as the amount of absorbed water progressively decreases, there is absence of a discontinuity



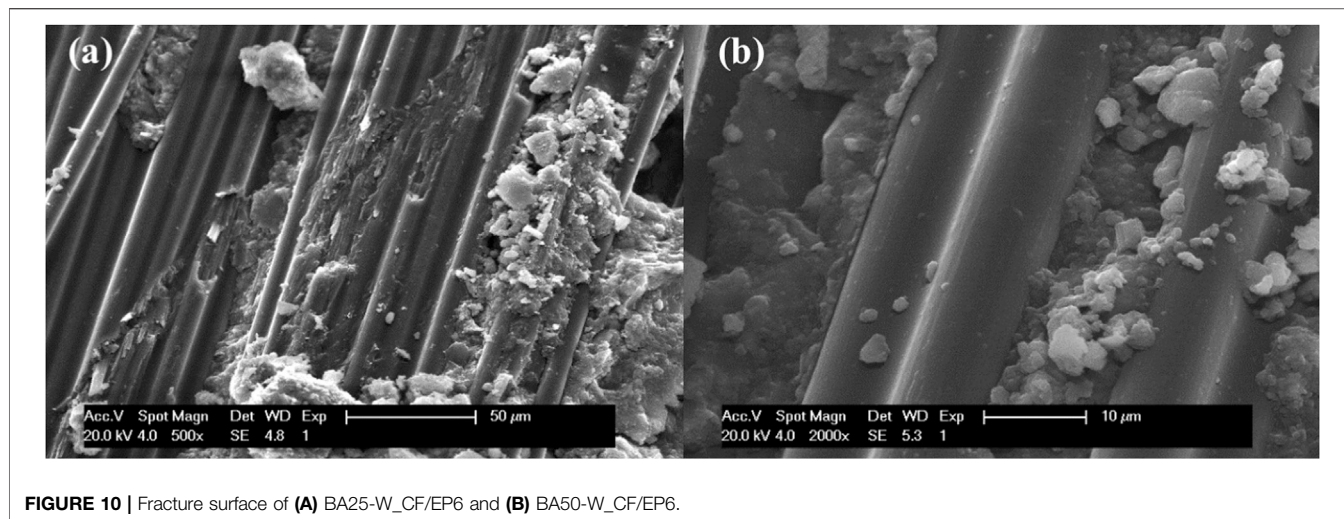


FIGURE 10 | Fracture surface of (A) BA25-W_CF/EP6 and (B) BA50-W_CF/EP6.

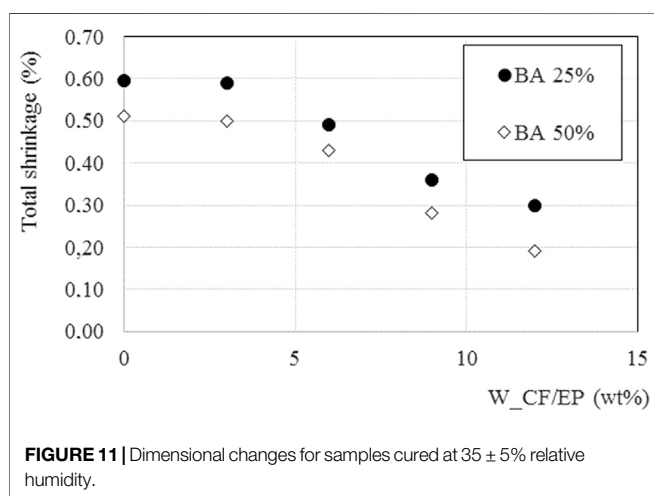


FIGURE 11 | Dimensional changes for samples cured at $35 \pm 5\%$ relative humidity.

between the waste and the matrix, suggesting an efficient adhesion between the different phases and the creation of a continuous interface transition zone between the cured epoxy and the ceramic matrix that can promote the increase in mechanical properties. The positive interaction is related to the presence of dipoles formed by C-O bonds in the resin interacting with ceramic matrix. The slight decrease in BA 50% compared with BA 25% can be explained considering the different total porosity of the two matrixes found by MIP analysis as observed in **Figure 3**. The same observation can explain the progressive reduction in the absorbed water as the amount of W_CF/EP increases. Indeed, a partial substitution of the porous phase, the matrix, with a non-porous fraction, the organic composite, takes place, decreasing the overall fraction of porosities.

The severed surfaces obtained by diamond sawing of the different samples (**Figures 5A–D**) again underline the absence of large voids (>1 mm) derived from insufficient workability, as was expected by visual inspection during casting operations. No differences at this magnification were found

between the different amounts of BA and consequently only 25 wt% BA loading is reported. No clusters of fibers were also visible from the Figures, implying that an efficient dispersion is obtained.

Figure 6 shows the flexural strength of the composites at 28 days of curing. As it can be observed, the increase in the amount of BA, from 25 to 50 wt%, decreases the mechanical properties of the composites. This is probably related to the presence, in the 50% samples, of a higher amount of porosities in the range from 0.02 to $0.4 \mu\text{m}$ with respect to the 25% BA composition as observed from the MIP measurements. This difference is possibly derived, as explained before, from the different reaction products generated (i.e., from the presence of C-A-S-H products) and also from the different kinetics of the binding reactions involving metakaolin and BA. However, the addition of W_CF/EP almost linearly increases the flexural strength of all the samples, confirming the positive effect of the fibers.

Figure 7 shows the plots reporting the force vs the deflection of all samples containing 50% of BA. For sake of brevity, only this set of specimens is reported. Along with the increase in flexural strength already discussed, a progressive increase in toughness takes place. In fiber-modified samples instead of one crack leading to the almost instantaneous overall fracture, a web of small cracks is formed leading to a postponed failure. Consequently, as the fully brittle behavior of the unmodified matrix is changed, higher amounts of energy can be absorbed as the amount of recycled composite increases. The mechanism supporting this effect is related to the progressive pull-out of the fibers from the matrix. The toughening effect of the fibers is reflected by the increase in the area beneath the plot.

Figure 8 reports the values of compressive strength of the investigated materials. This property is almost unaffected by the waste addition, both W_CP/EP and BA. Only at the highest amount of fibers, a slight reduction is found in samples, whereas at the lowest amounts, compressive strength slightly increases. Larger increases in compressive strength were found in other

researches, although with different conditions (Uddin and Shaikh, 2013; Bhutta et al., 2018).

The SEM analysis of mortars without W_CF/EP at different BA amounts is reported in **Figure 9**. Both the matrixes appear as compact without porosities. In the 50% BA matrix, some unreacted BA particles still showing sharp edges are visible. This confirms that at room temperature, the reactions leading to the geopolymerization of at least one fraction of BA are rather slow as previously observed (Uddin and Shaikh, 2013; Bhutta et al., 2018). **Figure 10** reports the morphology of the fractured surfaces derived from the flexural tests of samples modified with W_CF/EP. Some matrix particles adhere to the fibers, and no porosities are present at the interphase between matrix and wastes. This implies a fair interaction of the filler with the matrix, supporting the previous observations related to the amounts of absorbed water.

Indeed, it should also be underlined that no remarkable qualitative differences can be observed on changing the amount of BA in the matrix. Eventually, **Figure 11** reports the dimensional changes at 14 days for samples cured at $35 \pm 5\%$ relative humidity. A slight increase in the dimensional shrinkage of sample BA25-W_CF/EP can be observed when compared with BA50-W_CF/EP, probably on account of the overall higher porosity. Samples containing 3% of W_CF/EP show almost the same behavior as the unmodified matrixes, but further additions progressively increase the dimensional stability of the composites, an effect that has been found in conventional Portland cement materials by adding recycled carbon fibers (Wang et al., 2019).

It is important to underline from the results so far obtained that wastes derived from composite manufacturing can be recycled in the production of building materials without previous chemical or thermal treatments. The scraps can improve the mechanical behavior of metakaolin materials geopolymerized at low temperature. In this way, the use of low-energy consuming, low-impact products, where an economical value-added benefit is also achieved, can be successfully promoted.

CONCLUSIONS

The results of this research can thus be summarized as follows:

REFERENCES

- Akono, A. T., Koric, S., and Kriven, W. M. (2019). Influence of pore structure on the strength behavior of particle and fiber-reinforced metakaolin-based geopolymer composites. *Cem. Concr. Comp.* 104, 103361. doi:10.1016/j.cemconcomp.2019.103361
- Al-Mashhadani, M., Canpolat, O., Aygörmez, Y., Uysal, M., and Erdem, S. (2018). Mechanical and microstructural characterization of fiber reinforced fly ash based geopolymer composites. *Constr. Build. Mater.* 167, 505–513. doi:10.1016/j.conbuildmat.2018.02.061
- Aredes, F. G. M., Campos, T. M. B., Machado, J. P. B., Sakane, K. K., Thim, G. P., and Brunelli, D. D. (2015). Effect of cure temperature on the formation of metakaolinite-based geopolymer. *Ceram. Int.* 41, 7302–7311. doi:10.1016/j.ceramint.2015.02.022
- ASTM C1012/C1012M (2015). Standard test method for length change of hydraulic-cement mortars exposed to a sulfate solution, West Conshohocken, PA: ASTM International, 19428–2959.

- Metakaolin can be mixed with BA up to an amount of 50 wt %. The binder can still be activated at room temperature still showing even at the highest amount of BA, acceptable mechanical strengths.
- Untreated wastes derived from the production of carbon fiber epoxy composites have been homogeneously dispersed to formulate composites up to 12 weight %. Although the workability of the fresh mixtures decreases as the amount of waste increases, it is possible to cast mortars without high-dimension porosities. Microstructural analysis discloses a fair interaction between the fibers still surrounded by the epoxy coating and the matrix.
- CF/epoxy wastes increase the flexural strength of all the composites and drive their fracture from a brittle behaviour to a semiductile one. The compressive strength is practically unaffected by carbon fibers addition. Moreover, the addition of the fibrous wastes increases the dimensional stability of the composites.

DATA AVAILABILITY STATEMENT

All datasets presented in this study are included in the article.

AUTHOR CONTRIBUTIONS

SM: conceptualization, methodology, validation, investigation, resources, data curation, visualization, writing original draft preparation, and editing. IL: methodology, validation, and resources. GM: investigation, data curation, and visualization. AS: conceptualization, methodology, validation, investigation, resources, data curation, visualization, writing original draft preparation and editing, and supervision.

ACKNOWLEDGMENTS

The authors acknowledge the support of Lorenzo Lipparini (REGLASS) for providing CF/EP composites.

- Bai, T., Song, Z., Wang, H., Wu, Y., and Huang, W. (2019). Performance evaluation of metakaolin geopolymer modified by different solid wastes. *J. Clean. Prod.* 226, 114–121. doi:10.1016/j.jclepro.2019.04.093
- Bhutta, A., Farooq, M., and Banthia, N. (2018). Matrix hybridization using waste fuel ash and slag in alkali-activated composites and its influence on maturity of fibre-matrix bond. *J. Clean. Prod.* 177, 857–867. doi:10.1016/j.jclepro.2018.01.001
- Boca Santa, R. A. A., Soares, C., and Gracher Riella, H. (2016). Geopolymers with a high percentage of bottom ash for solidification/immobilization of different toxic metals. *J. Hazard. Mater.* 318, 145–153. doi:10.1016/j.jhazmat.2016.06.059
- Boca Santa, R. A. A., Soares, C., and Gracher Riella, H. (2017). Geopolymers obtained from bottom ash as source of aluminosilicate cured at room temperature. *Constr. Build. Mat.* 157, 459–466. doi:10.1016/j.conbuildmat.2017.09.111
- Borges, P. H. R., Banthia, N., Alcamand, H. A., Vasconcelos, W. L., and Nunes, E. H. M. (2016). Performance of blended metakaolin/blastfurnace slag alkali-activated mortars. *Cem. Concr. Comp.* 71, 42–52. doi:10.1016/j.cemconcomp.2016.04.008

- Chen, P., Feng, B., Lin, Y., and Lin, C. (2019). Solidification and stabilization of sewage sludge and MSWI bottom ash for beneficial use as construction materials. *J. Mater. Civ. Eng.* 31(1), 04018351. doi:10.1061/(ASCE)MT.1943-5533.0002572
- Chen, Z., and Yang, E. (2017). Early age hydration of blended cement with different size fractions of municipal solid waste incineration bottom ash. *Constr. Build. Mater.* 15, 880–890. doi:10.1016/j.conbuildmat.2017.09.063
- De Vargas, A. S., Dal Molin, D. C. C., Vilela, A. C. F., da Silva, F. J., Pavão, B., and Veit, H. (2011). The effects of Na₂O/SiO₂ molar ratio, curing temperature and age on compressive strength, morphology and microstructure of alkali-activated fly ash-based geopolymers. *Cem. Concr. Comp.* 33(6), 653–660. doi:10.1016/j.cemconcomp.2011.03.006
- Farooq, M., Bhutta, A., and Banthia, N. (2019). Tensile performance of eco-friendly ductile geopolymer composites (EDGC) incorporating different micro-fibers. *Cem. Concr. Comp.* 103, 183–192. doi:10.1016/j.cemconcomp.2019.05.004
- Guo, X., Shi, H., and Wei, X. (2017). Pore properties, inner chemical environment, and microstructure of nano-modified CFA-WBP (class C fly ash-waste brick powder) based geopolymers. *Cem. Concr. Comp.* 79, 53–61. doi:10.1016/j.cemconcomp.2017.01.007
- Huang, G., Ji, Y., Li, J., Hou, Z., and Jin, C. (2018). Use of slaked lime and Portland cement to improve the resistance of MSWI bottom ash-GBFS geopolymer concrete against carbonation. *Constr. Build. Mater.* 166, 290–300. doi:10.1016/j.conbuildmat.2018.01.089
- Kuo, W. T., Liu, C. C., and Su, D. S. (2013). Use of washed municipal solid waste incinerator bottom ash in pervious concrete. *Cem. Concr. Comp.* 37 (1), 328–335. doi:10.1016/j.cemconcomp.2013.01.001
- Lancellotti, I., Cannio, M., Bollino, F., Catauro, M., and Leonelli, C. (2015). Geopolymers: an option for the valorization of incinerator bottom ash derived “end of waste”. *Ceram. Int.* 41, 2116–2123. doi:10.1016/j.ceramint.2014.10.008
- Lancellotti, I., Ponzoni, C., Barbieri, L., and Leonelli, C. (2013). Alkali activation processes for incinerator residues management. *Waste Manag.* 33, 1740–1749. doi:10.1016/j.wasman.2013.04.013
- Lancellotti, I., Ponzoni, C., Bignozzi, M., Barbieri, L., and Leonelli, C. (2014). Incinerator BA and Ladle slag for geopolymers preparation. *Waste Bio. Valor.* 5, 393–401. doi:10.1007/s12649-014-9299-2
- Li, X., Lv, Y., Ma, B., Chen, Q., Yin, X., and Jian, S. (2012). Utilization of municipal solid waste incineration bottom ash in blended cement. *J. Clean. Prod.* 32, 96–100. doi:10.1016/j.jclepro.2012.03.038
- Logesh Kumar, M., and Revathi, V. (2016). Metakaolin bottom ash blend geopolymer mortar – a feasibility study. *Constr. Build. Mater.* 114, 1–5. doi:10.1016/j.conbuildmat.2016.03.149
- Luna-Galiano, Y., Leiva, C., Villegas, R., Arroyo, F., Vilches, L., and Fernández-Pereira, C. (2018). Carbon fiber waste incorporation in blast furnace slag geopolymer-composites. *Mater. Lett.* 233, 1–3. doi:10.1016/j.matlet.2018.08.099
- Rovnaník, P. (2010). Effect of curing temperature on the development of hard structure of metakaolin-based geopolymer. *Constr. Build. Mater.* 24, 1176–1183. doi:10.1016/j.conbuildmat.2009.12.023
- Saccani, A., Manzi, S., Lancellotti, I., and Lipparini, L. (2019). Composites obtained by recycling carbon fibre/epoxy composite wastes in building materials. *Constr. Build. Mater.* 204, 296–302. doi:10.1016/j.conbuildmat.2019.01.216
- Saccani, A., Sandrolini, F., Andreola, F., Lancellotti, I., Barbieri, L., and Corradi, A. (2005). Influence of the pozzolanic fraction obtained from vitrified bottom ashes from MSWI on the properties of cementitious composites. *Mater. Struct.* 38, 367–371. doi:10.1007/BF02479303
- Saccani, A., Sandrolini, F., Barbieri, L., and Lancellotti, I. (2001). Structural studies and electrical properties of re-cycled glasses from glass and incinerator wastes. *J. Mater. Sci.* 36, 2173–2177. doi:10.1023/A:1017539932421
- Sha, D., Pan, B., and Sun, Y. (2020). A novel raw material for geopolymers: coal-based synthetic natural gas slag. *J. Clean. Prod.* 262, 121238. doi:10.1016/j.jclepro.2020.121238
- Silva, R. V., de Brito, J., Lynn, C. J., and Dhir, R. K. (2017). Use of municipal solid waste incineration bottom ashes in alkali-activated materials, ceramics and granular applications: a review. *Waste Manag.* 68, 207–220. doi:10.1016/j.wasman.2017.06.043
- Sun, Z., and Vollpracht, A. (2019). One year geopolymerisation of sodium silicate activated fly ash and metakaolin geopolymers. *Cem. Concr. Comp.* 95, 98–110. doi:10.1016/j.cemconcomp.2018.10.014
- Tang, P., Florea, M., Spiesz, P., and Brouwers, H. (2016). Application of thermally activated municipal solid waste incineration (MSWI) bottom ash fines as binder substitute. *Cem. Concr. Comp.* 70, 194–205. doi:10.1016/j.cemconcomp.2016.03.015
- Uddin, F., and Shaikh, A. (2013). Review of mechanical properties of short fibre reinforced geopolymer composites. *Constr. Build. Mater.* 43, 37–49. doi:10.1016/j.conbuildmat.
- UNI 7699 (2005). *Testing hardened concrete. Determination of water absorption at atmospheric pressure*, Milano, Italy: Ente Nazionale Italiano di Unificazione.
- Vilaplana, J. L., Baeza, F. J., Galao, O., Alcocel, E. G., Zornoza, E., and Garces, P. (2016). Mechanical properties of alkali activated blast furnace slag pastes reinforced with carbon fibers. *Constr. Build. Mater.* 116, 63–71. doi:10.1016/j.conbuildmat.2016.04.066
- Wang, Y., Zhang, S., Li, G., and Shi, X. (2019). Effects of alkali treated recycled carbon fiber on the strength and free drying shrinkage of cementitious mortar. *J. Clean. Prod.* 228, 1187–1195. doi:10.1016/j.jclepro.2019.04.295
- Wongsa, A., Boonserm, K., Waisurasingha, C., Sata, V., and Chindaprasirt, P. (2017). Use of municipal solid waste incinerator (MSWI) bottom ash in high calcium fly ash geopolymer. *J. Clean. Prod.* 148, 49–59. doi:10.1016/j.jclepro.2017.01.147
- Zhu, W., Chen, X., Struble, L. J., and Yang, E.-H. (2018). Characterization of calcium containing phases in alkali-activated municipal solid waste incineration bottom ash binder through chemical extraction and deconvoluted Fourier transform infrared spectra. *J. Clean. Prod.* 192, 782–789. doi:10.1016/j.jclepro.2018.05.049

Conflict of Interest: The authors declare that the research was conducted in the absence of any commercial or financial relationships that could be construed as a potential conflict of interest.

Copyright © 2020 Manzi, Lancellotti, Masi and Saccani. This is an open-access article distributed under the terms of the Creative Commons Attribution License (CC BY). The use, distribution or reproduction in other forums is permitted, provided the original author(s) and the copyright owner(s) are credited and that the original publication in this journal is cited, in accordance with accepted academic practice. No use, distribution or reproduction is permitted which does not comply with these terms.